Ordering in PbSe Quantum Dot Superlattices Investigated by Anomalous X-Ray Diffraction

R.T. Lechner, G. Springholz, T. U. Schülli, V. Holy, J. Stangl, A. Raab and G. Bauer
Institut für Halbleiterphysik, Universität Linz, A-4040 Linz, Austria

Anomalous x-ray diffraction is used to investigate self-organized three dimensional PbSe quantum dot lattices formed by multilayer heteroepitaxial growth. Using a short-range dot ordering model in combination with a finite domain size, the ordering parameters are determined from the x-ray spectra. It is shown that the variance of the nearest-neighbor distances is significantly smaller and the laterally ordered domain size larger for the case of three dimensional trigonal PbSe dot lattices with *fcc*-stacking as compared to those with three dimensional hexagonal dot arrangement.

Introduction

High-resolution x-ray diffraction is a powerful tool for investigation of vertical and lateral correlations in three dimensional self-assembled quantum dots structures [1] – [3] obtained by multilayer heteroepitaxial growth. These correlations are caused by the elastic dot interactions [4], [5]. This not only results in a significant narrowing of the size distribution [6], but also provides an effective means for tuning the size and spacing of the dots by changes in the superlattice period [1], [7]. For different material systems, different ordered dot arrangements have been observed [1] – [5], which is due to the strong dependence of the dot interactions on the growth orientation as well as on the anisotropy of the elastic material properties [7]. The PbSe/ $Pb_{1-x}Eu_xTe$ system is unique in this respect because different interlayer correlations can be achieved in the superlattices by changes in the spacer thickness [8], dot size, or growth temperature [9].

In the present work, we employ anomalous x-ray diffraction with synchrotron radiation to drastically enhance the chemical contrast in multilayers by tuning the wavelength close to an inner shell absorption resonance [3]. This technique is applied to determine the ordering parameters of differently stacked self-assembled PbSe quantum dot lattices fabricated by molecular beam epitaxy based on the combination of a short-range order model with a finite domain size. As a result, it is shown that the lateral ordering is significantly better for *fcc*-stacked PbSe dot superlattices with 3D trigonal dot structure as compared to those with 3D hexagonal dot arrangement. This is due to the more efficient ordering mechanism based on the elastic interlayer dot interactions.

Experimental and Results

The samples were grown by molecular beam epitaxy onto on (111) BaF_2 substrates. Each superlattice stack (SL) consists of 50 to 60 periods of 5 monolayers (ML) PbSe alternating with $Pb_{1-x}Eu_xTe$ spacer layers with x_{Eu} = 8%. Due to the corresponding -5.4% lattice mismatch, strain-induced coherent islands are formed in each PbSe layer when its thickness exceeds 1.5 ML. For the investigation of the ordering process as a function of the PbEuTe spacer layer thickness, a series of samples was prepared with spacer thicknesses d_s varying from 80 to 500 Å. After growth, the final PbSe dot layer

was characterized by atomic force microscopy (AFM). To analyze the lateral and vertical dot correlations anomalous coplanar high-resolution x-ray diffraction is used at a very low energy of 2400eV, where the x-ray wavelength is tuned to the Pb M-shell to suppress the scattering of the (111) reflection of the matrix material. These measurements were performed with an in-vacuum diffractometer at the ID 1 beamline of the European synchrotron radiation facility in Grenoble and high resolution reciprocal space maps (RSMs) were recorded for all samples around the (111) Bragg reflection.

Here, we focus on four different superlattice samples with a spacer thickness of 104, 164, 214, and 454 Å for sample A to D, respectively. The (111) anomalous reciprocal space maps are shown in Fig. 1 (a) – (d) with the primary beam along the [$\underline{1}$01] azimuthal direction. Clearly, for all samples a large number of satellite peaks is observed both in the q_z direction along the surface normal, as well as in the direction q_x parallel to the surface. This clearly reflects the excellent order of the dots both vertically and laterally. However, whereas for samples A to C with thin spacer layers the lateral satellites are all aligned parallel to the q_x direction, the satellites for sample D are aligned in a direction inclined by 38° to the surface (dashed lines in Fig. 1). This indicates that in the latter case, the dots form a 3D trigonal dot lattice with *fcc*-like *ABCABC* stacking [1], whereas the dots for the other sample are aligned on top of each other in the vertical growth direction, corresponding to an overall 3D hexagonal dot arrangement [8].

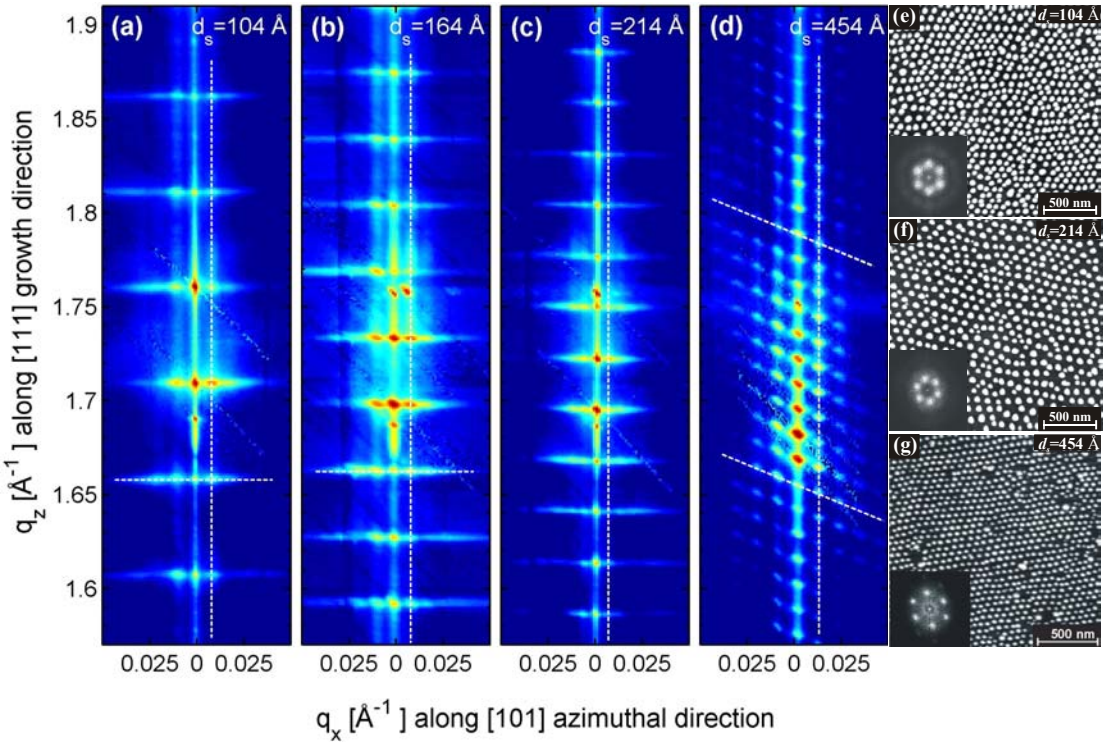

Fig. 1: (111) Reciprocal space maps (a) – (d) and atomic force microscopy images (e)-(g) of PbSe dot superlattice samples A - D with different PbEuTe spacer layers d_s = 104, 164, 214, 454 Å, respectively. The satellite arrangement indicates a 3D hexagonal dot lattice for (a) – (c) and 3D trigonal dot lattice for (d). The dashed lines mark the positions of the line scans along the q_x and the q_z direction used for the analysis of the order parameters.

To determine the quality of the dot ordering, diffraction line scans representing cross-sections of the reciprocal space maps in various q directions parallel (q_x) or perpen-

dicular (q_z) to the surface were recorded as indicated by the dashed lines in Fig. 1. Figure 2 shows the q_x-line scans along the lateral superlattice satellite peaks for the samples B and D. For comparison, in Fig. 2 (a) a line scan of sample B is included recorded at a 1.5 Å wavelength at the ROBL beamline. The improved contrast of the lateral dot satellite peaks for the longer wavelength is clearly visible in Fig. 2 (a) and (b).

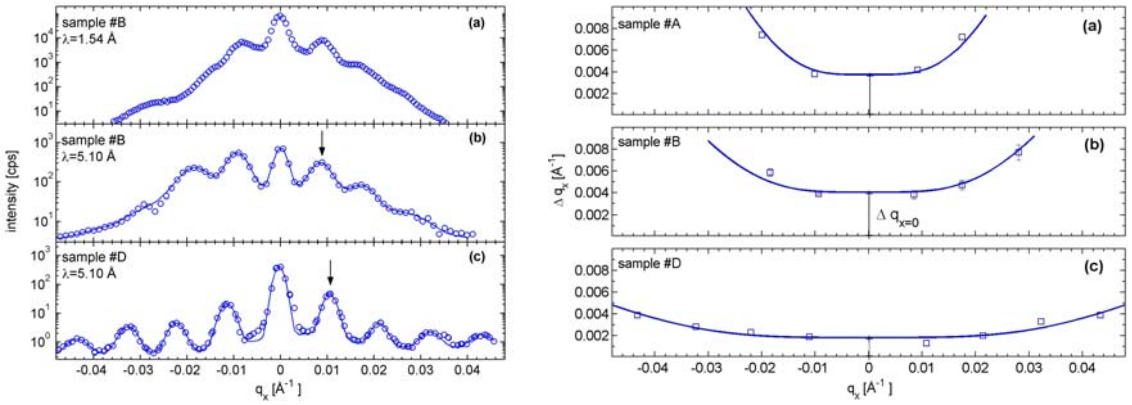

Fig. 2: *Left hand side*: Cross-sectional line scans of the XRD maps along the q_x direction for the vertically aligned dot sample B recorded with an x-ray wavelength of 1.5 Å (a) and 5.1 Å (b). The same is plotted in (c) for the *ABCABC* stacked sample D. The measured data (circles) are fitted with Gaussians with adjustable width (solid line). *Right hand side*: measured (symbols) and calculated (solid lines) FWHM Δq_x values of the peaks plotted over q_x. From the fits (solid lines), a variance σ_L and a domain size *M* of $\sigma_L = \pm 15\%$ and $M \approx 2$ is obtained for sample A, $\sigma_L = \pm 10\%$ and $M \approx 2$ for B, and $\sigma_L = \pm 5$ % and $M \approx 5$ for sample C.

From the spacing of these lateral satellite peaks, the lateral in-plane dot distances *L* within the layers can be determined. For the vertically aligned samples A to C, respective *L* values of 780, 850 and 950 Å are obtained, as compared to *L* = 670 Å for the *fcc*-stacked superlattice of sample D, in good agreement to the results obtained by AFM.

For the quantitative analysis of the order parameters, the full width at half maximum (FWHM) of the satellite peaks in q_x and q_z direction were determined as a function of the scattering vector *q*. This was achieved by fitting the cross-sectional line scans with Gaussians with adjustable width (solid lines in Fig. 2). To account for the broadening due the finite instrumental resolution, these values were corrected with the measured FWHMs of the PbSe-buffer peaks. The corrected FWHM, plotted on the right hand side of Fig. 2 as a function of q_x then represents the peak broadening caused by deviations of the ordered dot arrangement from an ideal perfect 3D lattice. Clearly for all samples the Δq_x half widths increase with increasing q_x scattering vector.

To analyze this behavior, we have adopted a model of short range ordering in the dot samples caused by the interlayer dot interactions during growth [2]. As the nature of the ordering is different perpendicular and parallel to the growth direction, we distinguish between the lateral correlations of the in-plane lateral dot positions (LL-correlation), the vertical correlations of the lateral dot positions (VL-correlation) and the vertical correlations of the vertical dot positions (VV-correlation). Assuming a short range order (SRO) model [2] for each correlation type, we can derive the lateral (Δq_x) and vertical (Δq_z) FWHM of the intensity satellite maxima as a function of the q_x position parallel to sample surface and the q_z position normal to the surface relative to the central 0^{th} order peak within the reciprocal scattering plane as:

$$\Delta q_x \approx \sqrt{\left(\frac{1}{L}(q_x^2\sigma_L^2)\right)^2 + M^2};\ \Delta q_z \approx \frac{1}{D}(q_x^2\,\sigma_{DL}^2 + q_z^2\sigma_D^2)\ \text{ with }\ M \approx \frac{2\pi}{\Delta q_{x=0}}\cdot\frac{1}{L} \qquad (1)$$

where *D* and *L* are the average vertical, respectively, lateral separation of the dots. In this expression, σ_D characterizes the degree of VV-correlations, σ_{DL} the degree of VL-correlations and σ_L the degree of LL-correlations in the samples in terms of the dispersion of the nearest neighbor dot-dot separations and *M* characterizes the finite domain size. For Δq_z we do not find a dependence of the values on q_z. Therefore, the VV-correlation along the superlattice growth axis is nearly perfect and is limited only by the stability of the epitaxial growth process. From the mean Δq_z values we derive a VL-correlation of the dot positions of about 25 times D_{SL} for the three vertically aligned samples, whereas for the sample with *fcc*-stacking we obtain a VL-correlation of only 7 times the SL period. This proves that the *vertical* ordering of the dots is more efficient in the 3D hexagonal samples, which is due to the fact that the strength of the elastic interactions in these samples is much stronger due to the smaller spacer thickness.

As is indicated by the solid lines in on the right hand side of Fig. 2, the q_x dependence of the Δq_x FWHM shows approximately a parabolic behavior. From the fits of the data using Eq. (1) we obtain σ_L values of 117, 86 and 36 Å for the samples A, B and D, respectively. Thus, the relative variance of the nearest neighbor lateral dot distance for the 3D hexagonal samples A and B is ±15 % and ±10 %, respectively. In contrast, for the 3D trigonal sample D with L = 670 Å we obtain a variance of only ±5 %, indicating the lateral ordering is substantially better than for the 3D hexagonal dot samples. This agrees with the observation that the width of the lateral satellites of the trigonal dot sample is much smaller as compared to that of the 3D hexagonal dot samples (see Fig. 2). The same general trend applies also for the domain size values *M,* for which a value of $M \approx 2$ is obtained for the vertically aligned samples A and B, whereas a much larger value of $M \approx 5$ is obtained for sample D with *fcc*- stacking.

Conclusions

In conclusion, anomalous high resolution x-ray diffraction is a powerful technique for investigation of the ordering parameters of 3D quantum dot multilayers and superlattices. Exploiting the advantages of anomalous diffraction we were able to enhance the scattering contrast between the PbSe dots and the matrix material to record a large number of satellite peaks for detailed analysis. We have obtained information not only on the different kinds of 3D ordering mechanisms; we can also determine the quality of the lateral and vertical correlation of the dot positions. This work was supported by the FWF, GME and the Academy of Science (APART) of Austria.

References

[1] G. Springholz, V. Holy, M. Pinczolits, and G. Bauer, Science **282**, 734-737 (1998).

[2] V. Holý, J. Stangl, G. Springholz, M. Pinczolits, G. Bauer, I.Kegel, and T.H. Metzger, Physica B **283**, 65-68 (2000).

[3] T.U. Schülli, J. Stangl, Z. Zhong, R.T. Lechner, M. Sztucki, T.H. Metzger, and G.Bauer, Phys. Rev. Lett. **90**, 066105 (2003).

[4] Q. Xie, A. Madhukar, P. Chen, N. Kobayashi, Phys. Rev. Lett. **75**, 2542 (1995).

[5] J. Tersoff, C. Teichert, and M. G. Lagally, Phys. Rev. Lett. **76**, 1675 (1996).

[6] M. Pinczolits, G. Springholz, and G. Bauer, Phys. Rev. B **60**, 11524 (1999).

[7] V. Holy, G. Springholz, M. Pinczolits, G. Bauer, Phys. Rev. Lett. **83**, 356 (1999).

[8] G. Springholz, M. Pinczolits, P. Mayer, V. Holy, G. Bauer, H. H. Kang, and L. Salamanca-Riba, Phys. Rev. Lett. **84**, 4669 (2000).

[9] G. Springholz, A. Raab, R. T. Lechner, V. Holy, Appl. Phys. Lett. **82**, 799 (2003).

[10] A.Raab, R. T. Lechner, and G. Springholz, Phys. Rev. B **67**, 165321 (2003).